Study of P and CP symmetries in $\Xi_c^+ \to \Xi^-\pi^+\pi^+$ at electron-positron collider

Yunlu Wang (王云路)[1†] Yunlong Xiao (肖云龙)[1‡] Pengcheng Hong (洪鹏程)[2,4§] Ronggang Ping (平荣刚)[3,4¶]

[1]Key Laboratory of Nuclear Physics and Ion-beam Application (MOE) and Institute of Modern Physics, Fudan University, Shanghai 200433, China
[2]College of Physics, Jilin University, Changchun 130012, China
[3]University of Chinese Academy of Science, the Chinese Academy of Science, Beijing 100049, China
[4]Institute of High Energy Physics, the Chinese Academy of Science, Beijing 100049, China

Abstract: Symmetry studies represent one of the most promising frontiers in particle physics research. This investigation focuses on exploring P and CP symmetries in the charm system through the measurement of asymmetry decay parameters in the three-body decay of Ξ_c^+. By incorporating electron and positron beam polarization effects and utilizing the helicity formalism, we characterize the decay of Ξ_c^+ and its secondary hyperons through asymmetry decay parameters. The complete angular distribution formula for these decays is systematically derived. Our study evaluates the sensitivity of the asymmetry parameters for the $\Xi_c^+ \to \Xi^-\pi^+\pi^+$ decay channel under various data sample sizes and beam polarization scenarios. The findings establish a robust theoretical framework for future experimental studies at the Super Tau-Charm Facility, providing valuable insights for symmetry investigations in the charm sector.

Keywords: symmetry, polarization, baryon

DOI: 10.1088/1674-1137/ae15ed **CSTR:** 32044.14.ChinesePhysicsC.50023112

I. INTRODUCTION

Charge parity (CP) violation is one of the three fundamental conditions required to explain the matter-antimatter asymmetry observed in the universe [1]. In the Standard Model of particle physics, the quark dynamics are described by the Cabibbo-Kobayashi-Maskawa (CKM) mechanism [2, 3]. While the CP violation observed in the decays of K, B, and D mesons is well described by the CKM mechanism [4−10], it remains insufficient to account for the observed matter-antimatter asymmetry in the universe [11]. Given that the observable universe is predominantly composed of baryons, studying CP violation in baryon decays is crucial for understanding this asymmetry. Recent experimental advancements have provided compelling evidence for CP violation in Λ_b baryons. For instance, the evidence of CP violation in $\Lambda_b \to \Lambda K^+K^-$ [12] decay and the first observation of CP violation in the four-body decay of $\Lambda_b \to pK^-\pi^+\pi^-$ [13] have been reported at the LHCb experiment. However, current research on CP violation primarily focuses on Λ_b decays, making it challenging to directly compare theoretical predictions involving baryon decays without b-quarks. This highlights the need for exploring CP violation in other baryonic systems. The two-body decay processes of baryons can be parameterized using decay parameters α and $\bar{\alpha}$. Parity violation in baryons and anti-baryons is indicated by non-zero values of α and $\bar{\alpha}$ [14]. Experimentally, CP symmetry is tested by comparing the decay parameters of baryons and anti-baryons through the CP-odd observable $\mathcal{A}_{\rm CP} = (\alpha+\bar{\alpha})/(\alpha-\bar{\alpha})$ [15−19]. Here, α and $\bar{\alpha}$ represent the decay parameters of the baryon and anti-baryon, respectively. Non-zero measurements of α and $\mathcal{A}_{\rm CP}$ signify parity (P) and CP violations [20−24]. While two-body decays of baryons have been extensively studied, identifying new sources of CP violation in baryon decays without b-quarks is essential for elucidating this mystery and represents a critical frontier in CP violation research.

The Cabibbo-favored three-body decay of the charmed baryon, $\Xi_c^+ \to \Xi^-\pi^+\pi^+$, involves both external and internal W-emission modes, with decay amplitudes encompassing factorizable and non-factorizable contributions. The total branching fractions of $\Xi_c^+ \to \Xi^-\pi^+\pi^+$ and

Received 15 July 2025; Accepted 21 October 2025; Accepted manuscript online 22 October 2025

† E-mail: yunluwang20@fudan.edu.cn
‡ E-mail: xiaoyunlong@fudan.edu.cn (Corresponding author)
§ E-mail: hongpc@ihep.ac.cn
¶ E-mail: pingrg@ihep.ac.cn

its isospin channel $\Xi_c^+ \to \Xi^0\pi^0\pi^+$ are approximately 10%, making them the most probable decay modes [25]. Consequently, these channels are expected to yield abundant experimental data, facilitating the investigation of P and CP violations at future facilities, such as the Super Tau-Charm Facility (STCF) [26].

The parameters for three-body decays cannot be directly described by the Lee-Yang formalism [27]. Therefore, it is necessary to define analogous decay parameters through decay amplitudes to study P and CP violations. In electron-positron collisions, the threshold energy for the process $e^+e^- \to \Xi_c^+\bar{\Xi}_c^-$ is above 4.94 GeV. Both the upgraded BESIII experiment and the future STCF are expected to produce Ξ_c^+ and $\bar{\Xi}_c^-$ pairs. Precision measurements of the decay parameters for $\Xi_c^+ \to \Xi^-\pi^+\pi^+$ and its isospin process $\Xi_c^+ \to \Xi^0\pi^0\pi^+$ will provide critical insights to validate or exclude existing theoretical models and test isospin symmetry through comparative decay parameters.

The amplitude for decay $\Xi_c^+(\lambda_1) \to \Xi^-(\lambda_2)\pi^+\pi^+$ is expected to provide all information about spin and helicity of the particles. In the helicity formalism, the amplitude is model-independent and expressed by $B^J_\mu(\lambda_2,0,0)$, which encodes the sum of resonances in Eq. (2). Here, $J = 1/2$ is the spin of the mother particle, μ is its eigenvalue in the body-fixed z-axis, which can be $1/2$ or $-1/2$, and $\lambda_2 = \pm 1/2$ is the helicity of Ξ^-. Then, there are four degrees of freedom, namely $B^{\frac{1}{2}}_{\frac{1}{2}}(\frac{1}{2},0,0), B^{\frac{1}{2}}_{-\frac{1}{2}}(\frac{1}{2},0,0), B^{\frac{1}{2}}_{\frac{1}{2}}(-\frac{1}{2},0,0)$, and $B^{\frac{1}{2}}_{-\frac{1}{2}}(-\frac{1}{2},0,0)$, which are denoted by $B^\mu_{\lambda_2}$ for simplification.

Similarly, the production of Ξ_c^+ and decay of Ξ^- are also expressed in the helicity formalism, and the corresponding amplitudes are listed in Table 1. If the parity is conserved [28], the four amplitudes should satisfy the relations $B^+_{\frac{1}{2}} = -B^+_{-\frac{1}{2}}$ and $B^-_{\frac{1}{2}} = B^-_{-\frac{1}{2}}$. However, the weak decay process $\Xi_c^+ \to \Xi^-\pi^+\pi^+$ allows for parity violation. To characterize parity violation in this process, three asymmetry parameters can be defined by the following formulas:

$$\begin{aligned}\alpha_{\Xi_c^+} &= \frac{|B^+_{\frac{1}{2}}|^2 - |B^+_{-\frac{1}{2}}|^2}{|B^+_{\frac{1}{2}}|^2 + |B^+_{-\frac{1}{2}}|^2},\\ \beta_{\Xi_c^+} &= \frac{|B^-_{\frac{1}{2}}|^2 - |B^-_{-\frac{1}{2}}|^2}{|B^-_{\frac{1}{2}}|^2 + |B^-_{-\frac{1}{2}}|^2},\\ \gamma_{\Xi_c^+} &= \frac{|B^+_{\frac{1}{2}}|^2 + |B^+_{-\frac{1}{2}}|^2}{|B^-_{\frac{1}{2}}|^2 + |B^-_{-\frac{1}{2}}|^2}.\end{aligned} \tag{1}$$

They are extended definitions from the two-body decay, based on asymmetry parameters in terms of partial wave amplitudes from Lee-Yang [27] but in the helicity formalism. The parameter $\gamma_{\Xi_c^+}$ represents the relative magnitude of both types of degenerate amplitudes.

Table 1. Helicity angles and amplitudes in relative decays.

Decay	Helicity angle	Helicity amplitude
$\gamma^* \to \Xi_c^+(\lambda_1)\bar{\Xi}_c^-(\lambda_0)$	(θ_1,ϕ_1)	A_{λ_1,λ_0}
$\Xi_c^+(\lambda_1) \to \Xi^-(\lambda_2)\pi^+\pi^+$	(ϕ_2,θ_2,ψ_2)	$B^\mu_{\lambda_2}$
$\Xi^-(\lambda_2) \to \Lambda(\lambda_3)\pi^-$	(θ_3,ϕ_3)	F_{λ_3}
$\Lambda(\lambda_3) \to p(\lambda_4)\pi^-$	(θ_4,ϕ_4)	H_{λ_4}

The decay $\Xi_c^+ \to \Xi^-\pi^+\pi^+$ may include intermediate resonance processes from three two-body decays: $\Xi_c^+ \to \Xi(1530)^0\pi^+ \to \Xi^-\pi^+\pi^+$, $\Xi_c^+ \to \Xi(1620)^0\pi^+ \to \Xi^-\pi^+\pi^+$, and $\Xi_c^+ \to \Xi(1690)^0\pi^+ \to \Xi^-\pi^+\pi^+$. Among these, the first process is suppressed because the spin of $\Xi(1530)^0$ is 3/2. The intermediate states $\Xi(1620)^0$ and $\Xi(1690)^0$ are allowed and can also be described by our method. The amplitudes are model-independent and are relative to intermediate states by the following integration:

$$|B^\mu_{\lambda_2}|^2 = \int \mathrm{d}\Phi_3 |\tilde{B}^\mu_{\lambda_2}(m_{\Xi^-\pi^+}, m_{\Xi^-\pi'^+}, m_{\pi^+\pi'^+})|^2, \tag{2}$$

where $m_{\Xi^-\pi^+}$ and $m_{\Xi^-\pi'^+}$ are the invariant masses of Ξ^- with two pions, respectively, which are also treated as Dalitz plots variables [29]; the space $\mathrm{d}\Phi_3$ consists of the Euler angles given in Table 1; $m_{\pi^+\pi'^+}$ is the invariant mass of two pions. The integration can be estimated by using the Monte-Carlo method; however, this falls out of the scope of this study; therefore, we keep the amplitudes arbitrary for generality and clarify the magnitude and phase angle of an amplitude by denoting $B^+_{\lambda_2} = b^+_{\lambda_2} e^{i\zeta^+_{\lambda_2}}$. Thus, the four magnitudes can be rewritten in terms of the asymmetry parameters as

$$\begin{aligned}(b^+_{\frac{1}{2}})^2 &= 1,\\ (b^+_{-\frac{1}{2}})^2 &= \frac{1-\alpha_{\Xi_c^+}}{1+\alpha_{\Xi_c^+}},\\ (b^-_{\frac{1}{2}})^2 &= \frac{1+\beta_{\Xi_c^+}}{\gamma_{\Xi_c^+}(1+\alpha_{\Xi_c^+})},\\ (b^-_{-\frac{1}{2}})^2 &= \frac{1-\beta_{\Xi_c^+}}{\gamma_{\Xi_c^+}(1+\alpha_{\Xi_c^+})}.\end{aligned} \tag{3}$$

Analogous to Eq. (1), the asymmetry parameters $\alpha_{\bar{\Xi}_c^-}$, $\beta_{\bar{\Xi}_c^-}$, and $\gamma_{\bar{\Xi}_c^-}$ for the decay of the antibaryon $\bar{\Xi}_c^- \to \bar{\Xi}^+\pi^-\pi^-$ have similar expressions. With these parity parameters, the CP violation can be characterized by

$$\mathcal{A}_{\mathrm{CP}} = \frac{\alpha_{\Xi_c^+} + \alpha_{\bar{\Xi}_c^-}}{\alpha_{\Xi_c^+} - \alpha_{\bar{\Xi}_c^-}},$$

$$\mathcal{B}_{\rm CP} = \frac{\beta_{\Xi_c^+} + \beta_{\bar{\Xi}_c^-}}{\beta_{\Xi_c^+} - \beta_{\bar{\Xi}_c^-}},$$
$$C_{\rm CP} = \frac{\gamma_{\Xi_c^+} - \gamma_{\bar{\Xi}_c^-}}{\gamma_{\Xi_c^+} + \gamma_{\bar{\Xi}_c^-}}, \quad (4)$$

which have the advantage that the systematic uncertainties of production and detection asymmetries are largely canceled [30]. The parameters can be included in other expressions after inserting partial amplitudes. For example, the leading-power expansion of the first parameter is reduced to [15, 31]

$$\mathcal{A}_{\rm CP} \propto -\tan\Delta\delta \tan\Delta\phi, \quad (5)$$

where the relative strong phase $\Delta\delta$ depends on final states, and the weak phase $\Delta\phi$ stems from interference between amplitudes with different partial wave configurations in the same decay [32]. The amplitudes partially derive from tree and penguin diagrams such as the examples shown in Fig. 1, where the interfered CKM matrix elements $V_{cs}^* V_{ud} \times V_{cb}^* V_{tb} V_{ts}^* V_{ud}$ and their conjugations give rise to the non-zero phase $\Delta\phi$.

The tree diagram is Cabibbo-favored, while the penguin diagram is suppressed from off-diagonal elements $V_{cb}^* V_{ts}^*$. Following the measured values of the CKM matrix [25], the magnitude of the weak phase shift is approximately Im$[-(V_{cb}^* V_{tb} V_{ts}^* V_{ud})]$ and expected to be on the order of $O(10^{-4} \sim 10^{-5})$. Owing to the possible suppression of the strong phase, the magnitude of CP violation is expected to be smaller than the expected value, and the interference effect between the two figures in Fig. 1 also tends to suppress the observation of the violation. If CP violation enhances, it is attributed to a combination of direct CP violation and potential new physics contributions. To determine these effects, further measurements need to be performed at STCF in the future.

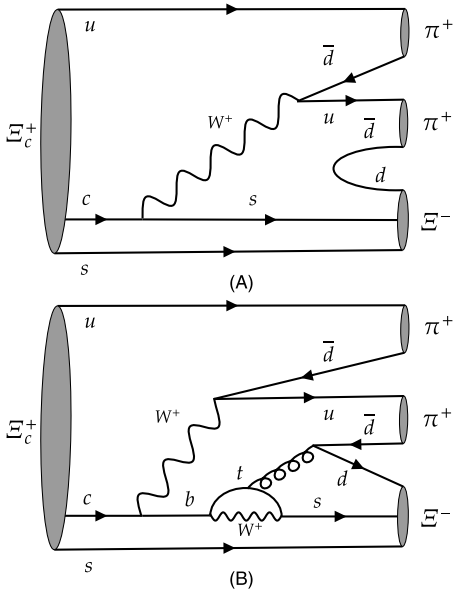

Fig. 1. Tree and penguin diagrams as examples for $\Xi_c^+ \to \Xi^-\pi^+\pi^+$ decay.

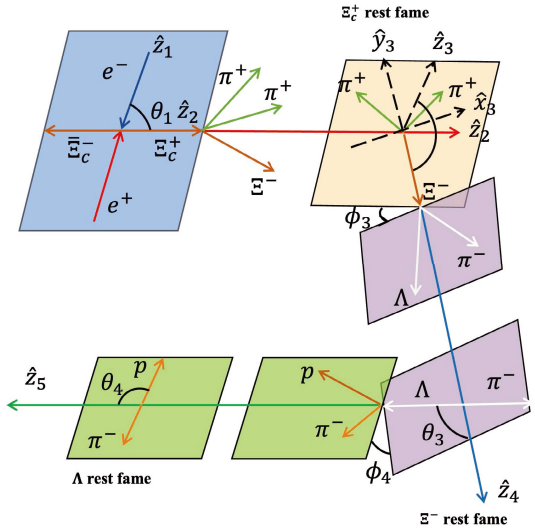

Fig. 2. (color online) Definition of helicity frame at e^+e^- collider.

II. HELICITY SYSTEM

In this analysis, we adopt a helicity frame to describe the decay chain [28]. The helicity angles and amplitudes of the $\Xi_c^+\bar{\Xi}_c^-$ production and decay are listed in Table 1, and the corresponding angles are also shown in Fig. 2. The momentum p_i is obtained by boosting particle i to the rest frame of its mother particle.

The angle between the Ξ_c^+ production and the collision plane is defined as ϕ_1. For the three-body decay of $\Xi_c^+ \to \Xi^-\pi^+\pi^+$, the Euler angles $(\phi_2, \theta_2, \psi_2)$ are used. The system is rotated from $\hat{z}_2$ to $\hat{z}_3$ following the ZYZ convention. In Ξ^- decays, a rotation from $\hat{z}_3$ to $\hat{z}_4$ is needed. Owing to the rotational invariance of helicity, this rotation operation does not introduce any additional modifications. In fact, the angle ψ_2 will not contribute to the integrated cross sections that we are interested in, and the pion selection does not alter amplitudes given that the spin of the meson is zero.

III. ANGULAR DISTRIBUTIONS

The spin and polarization information of particles can be encoded in the spin density matrix (SDM) [33, 34]. The SDM of spin-1/2 particles such as Ξ_c^+ is expressed by a 2×2 matrix:

$$\rho^{\Xi_c^+} = \frac{\mathcal{P}_0}{2}\begin{pmatrix} 1+\mathcal{P}_z & \mathcal{P}_x - i\mathcal{P}_y \\ \mathcal{P}_x + i\mathcal{P}_y & 1-\mathcal{P}_z \end{pmatrix},$$

where $\mathcal{P}_0$ carries the unpolarized information. Polarization $\mathcal{P}_z$ represents the longitudinal part, while the information of transverse polarization is encoded by $\mathcal{P}_x$ and $\mathcal{P}_y$. To obtain their explicit expressions, transfer functions starting from the initial collision will be solved in the following sections.

A. Ξ_c^+ production on e^+e^- collider

The SDM of Ξ_c^+ from polarized virtual photon can be expressed as

$$\rho^{\Xi_c^+}_{\lambda_1,\lambda_1'} \propto \sum_{\lambda,\lambda_0} \rho^{\gamma^*}_{\lambda,\lambda'} D^{1*}_{\lambda,\lambda_1-\lambda_0}(\phi_1,\theta_1,0) \times D^{1}_{\lambda',\lambda_1'-\lambda_0}(\phi_1,\theta_1,0) A_{\lambda_1,\lambda_0} A^*_{\lambda_1',\lambda_0}, \tag{6}$$

where $D^J_{\lambda_j,\lambda_k}$ is the Wigner-D function. For polarized symmetric e^+e^- beams, if the transverse polarization information is considered, the SDM of photon is given by [35]

$$\rho^{\gamma^*}_{\lambda_0,\lambda_0'} = \frac{1}{2}\begin{pmatrix} 1 & 0 & p_T^2 \\ 0 & 0 & 0 \\ p_T^2 & 0 & 1 \end{pmatrix}, \tag{7}$$

where the range of transverse polarization p_T satisfies $0 < p_T < 1$. Considering Eq. (6) under parity conservation, we can obtain the unpolarized cross section, which depends on the polarization of virtual photon, that is

$$\mathcal{P}_0 = 1 + \alpha_c \cos^2\theta_1 + p_T^2 \alpha_c \sin^2\theta_1 \cos 2\phi_1 . \tag{8}$$

The constant $\frac{1}{2}|A_{\frac{1}{2},-\frac{1}{2}}|^2 + |A_{\frac{1}{2},\frac{1}{2}}|^2$ is suppressed given that it does not contribute to the final normalized cross sections. The angular distribution parameter α_c for $e^+e^- \to \Xi_c^+\bar{\Xi}_c^-$ is defined as

$$\alpha_c = \frac{|A_{\frac{1}{2},-\frac{1}{2}}|^2 - 2|A_{\frac{1}{2},\frac{1}{2}}|^2}{|A_{\frac{1}{2},-\frac{1}{2}}|^2 + 2|A_{\frac{1}{2},\frac{1}{2}}|^2}. \tag{9}$$

The transverse and longitudinal polarizations of Ξ_c^+ are

$$\begin{aligned} \mathcal{P}_x &= \frac{-p_T^2\sqrt{1-\alpha_c^2}\sin\Delta_1\sin\theta_1\sin 2\phi_1}{1+\alpha_c\cos^2\theta_1 + p_T^2\alpha_c\sin^2\theta_1\cos 2\phi_1}, \\ \mathcal{P}_y &= \frac{\sqrt{1-\alpha_c^2}\sin\Delta_1\sin\theta_1\cos\theta_1(1-p_T^2\cos 2\phi_1)}{1+\alpha_c\cos^2\theta_1 + p_T^2\alpha_c\sin^2\theta_1\cos 2\phi_1}, \\ \mathcal{P}_z &= 0, \end{aligned} \tag{10}$$

where Δ_1 represents the phase angle difference, that is, $\Delta_1 = \zeta_{\frac{1}{2},-\frac{1}{2}} - \zeta_{\frac{1}{2},\frac{1}{2}}$. In symmetric electron-positron collision experiments, the transverse polarization of the positron and electron beams directly influences the transverse polarization of Ξ_c^+ as well as $\bar{\Xi}_c^-$. Although measured values of the parity parameter of this process are lacking, in the following sections we assume $\alpha_c = 0.7$ and $\Delta_1 = \pi/6$, which are close to the measurements of strange baryons [36].

B. $\Xi_c^+(\lambda_1) \to \Xi^-(\lambda_2)\pi^+\pi^+$

The information regarding the parity violation of this three-body decay is carried by the SDM of Ξ^-, which is given by the transfer equation:

$$\rho^{\Xi^-}_{\lambda_2,\lambda_2'} \propto \sum_{\lambda_1,\lambda_1',\mu} \rho^{\Xi_c^+}_{\lambda_1,\lambda_1'} D^{\frac{1}{2}*}_{\lambda_1,\mu}(\phi_2,\theta_2,\psi_2) \times D^{\frac{1}{2}}_{\lambda_1',\mu}(\phi_2,\theta_2,\psi_2) B^{\mu}_{\lambda_2} B^{\mu*}_{\lambda_2'}, \tag{11}$$

where μ is the z-component of the angular momentum of Ξ_c^+ whose quantization axis itself rotates under the rotation of the system. After summing all combinations and implementing simplifications, the polarization operators of Ξ^- reduce to

$$\begin{aligned} \mathcal{P}_0^{\Xi^-} &= \frac{\mathcal{P}_0}{2}\left(f_+^{\Xi^-} + f_-^{\Xi^-}\mathcal{P}_{xy}\sin\theta_2\right), \\ \mathcal{P}_0^{\Xi^-}\mathcal{P}_z^{\Xi^-} &= \frac{\mathcal{P}_0}{2}\left(g_+^{\Xi^-} + g_-^{\Xi^-}\mathcal{P}_{xy}\sin\theta_2\right), \\ \mathcal{P}_0^{\Xi^-}\mathcal{P}_x^{\Xi^-} &= \mathcal{P}_0\Big[\cos\Delta^+\left(1+\mathcal{P}_{xy}\sin\theta_2\right) b^+_{\frac{1}{2}} b^+_{-\frac{1}{2}} \\ &\quad + \cos\Delta^-\left(1-\mathcal{P}_{xy}\sin\theta_2\right) b^-_{\frac{1}{2}} b^-_{-\frac{1}{2}}\Big], \\ \mathcal{P}_0^{\Xi^-}\mathcal{P}_y^{\Xi^-} &= -\mathcal{P}_0\Big[\sin\Delta^+\left(1+\mathcal{P}_{xy}\sin\theta_2\right) b^+_{\frac{1}{2}} b^+_{-\frac{1}{2}} \\ &\quad + \sin\Delta^-\left(1-\mathcal{P}_{xy}\sin\theta_2\right) b^-_{\frac{1}{2}} b^-_{-\frac{1}{2}}\Big], \end{aligned} \tag{12}$$

where the functions $f_\pm^{\Xi^-}$ and $g_\pm^{\Xi^-}$ carry the dynamical information of the decay via Eq. (3) and are defined by

$$\begin{aligned} f_\pm^{\Xi^-} &= (b^+_{\frac{1}{2}})^2 + (b^+_{-\frac{1}{2}})^2 \pm \left[(b^-_{\frac{1}{2}})^2 + (b^-_{-\frac{1}{2}})^2\right], \\ g_\pm^{\Xi^-} &= (b^+_{\frac{1}{2}})^2 - (b^+_{-\frac{1}{2}})^2 \pm \left[(b^-_{\frac{1}{2}})^2 - (b^-_{-\frac{1}{2}})^2\right]. \end{aligned} \tag{13}$$

Interestingly, $g_\pm^{\Xi^-} = 0$ when parity is conserved. The transverse information from Ξ_c^+ is involved via the definition $\mathcal{P}_{xy} = \mathcal{P}_x\cos\phi_2 + \mathcal{P}_y\sin\phi_2$. The transverse polarizations of Ξ^- depend on phase differences defined by $\Delta_\pm = \zeta^-_{\pm\frac{1}{2}} - \zeta^+_{\pm\frac{1}{2}}$ and $\Delta^\pm = \zeta^\pm_{-\frac{1}{2}} - \zeta^\pm_{\frac{1}{2}}$, which lead to the relation $\Delta_+ - \Delta_- + \Delta^-\Delta^+ = 0$. The parity parameters for the three-body system adopted in $\Lambda_c^+ \to pK^-\pi^+$ decay [37] have other definitions as well; they can be related to our parameters as follows:

$$\begin{aligned}\mathcal{G}_0 =& \frac{\gamma^{\Xi_c^+}-1}{\gamma^{\Xi_c^+}+1},\\ \mathcal{G}_1 =& \kappa_-\sin\Delta_- + \kappa_+\sin\Delta_+,\\ \mathcal{G}_2 =& \kappa_-\cos\Delta_- + \kappa_+\cos\Delta_+,\end{aligned} \tag{14}$$

where

$$\kappa_\pm = \frac{\sqrt{(1\pm\alpha_{\Xi_c^+})(1\pm\beta_{\Xi_c^+})\gamma_{\Xi_c^+}}}{1+\gamma_{\Xi_c^+}}. \tag{15}$$

When parity is conserved, the values of parameters $\mathcal{G}_1$ and $\mathcal{G}_2$ cannot be determined directly owing to their undetermined phases in Eq. (14), while $\alpha_{\Xi_c^+} = \beta_{\Xi_c^+} = 0$, which provides more freedom for cross-testing of parity violations.

C. Cascade decays and joint angular distributions

The dominant processes for Ξ^- decays are $\Xi^- \to \Lambda\pi^-$ and $\Lambda \to p\pi^-$. Their helicity angles and amplitudes are defined in Sec. II, and the asymmetry parameter of the spin-1/2 baryons for the decay $\Xi^- \to \Lambda\pi^-$ can be defined as

$$\alpha_{\Xi^-} = \frac{|F_{\frac{1}{2}}|^2 - |F_{-\frac{1}{2}}|^2}{|F_{\frac{1}{2}}|^2 + |F_{-\frac{1}{2}}|^2}. \tag{16}$$

The parameter α_Λ for $\Lambda \to p\pi^-$ has a similar expression. The latest measurements of both parameters are $\alpha_{\Xi^-} = -0.367^{+0.005}_{-0.006}$ and $\alpha_\Lambda = 0.746 \pm 0.008$ from the Particle Data Group (PDG) [25]. By formalizing an equation similar to Eq. (11), the unpolarized and longitudinal parts of Λ can be derived:

$$\begin{aligned}\mathcal{P}_0^\Lambda =& \frac{2\mathcal{P}_0^{\Xi^-}}{1+\alpha_{\Xi^-}}\Big[1+\alpha_{\Xi^-}\cos\theta_3\mathcal{P}_z^{\Xi^-}\\ &+\alpha_{\Xi^-}\sin\theta_3\left(\cos\phi_3\mathcal{P}_x^{\Xi^-}+\sin\phi_3\mathcal{P}_y^{\Xi^-}\right)\Big],\end{aligned} \tag{17}$$

$$\begin{aligned}\mathcal{P}_0^\Lambda\mathcal{P}_z^\Lambda =& \frac{2\mathcal{P}_0^{\Xi^-}}{1+\alpha_{\Xi^-}}\Big\{\alpha_{\Xi^-}+\cos\theta_3\mathcal{P}_z^{\Xi^-}\\ &+\sin\theta_3\left(\cos\phi_3\mathcal{P}_x^{\Xi^-}+\sin\phi_3\mathcal{P}_y^{\Xi^-}\right)\Big\}.\end{aligned} \tag{18}$$

The proton SDM can be obtained in the same manner, and the angular distribution is given by $\mathcal{W} = \mathrm{Tr}\rho^p$, which is similar to Eq. (17) but expressed in terms of polarizations of Λ. Next, the distributions for helicity angles can be obtained by integrating out other angles, and the nontrivial distributions are

$$\frac{\mathrm{d}N}{\mathrm{d}\phi_1} \propto 1 + \alpha_c\frac{1+2p_T^2}{3}\cos2\phi_1, \tag{19}$$

$$\frac{\mathrm{d}N}{\mathrm{d}\cos\theta_1} \propto 1 + \alpha_c\cos^2\theta_1, \tag{20}$$

$$\frac{\mathrm{d}N}{\mathrm{d}\cos\theta_3} \propto 1 + \alpha_{\Xi^-}\frac{g_+^{\Xi^-}}{f_+^{\Xi^-}}\cos\theta_3, \tag{21}$$

$$\frac{\mathrm{d}N}{\mathrm{d}\cos\theta_4} \propto 1 + \alpha_{\Xi^-}\alpha_\Lambda\cos\theta_4, \tag{22}$$

where the distribution of $\cos\theta_1$ is free of beam polarization, the last distribution in Eq. (22) was reported in Ref. [25], and the distribution of $\cos\theta_2$ is flat. The distribution of $\cos\theta_3$ is affected by parity parameters of Ξ_c^+ through $g_+^{\Xi^-}/f_+^{\Xi^-} = (\beta_{\Xi_c^+} + \alpha_{\Xi_c^+}\gamma_{\Xi_c^+})/(1+\gamma_{\Xi_c^+})$. Plots of Eqs. (19) and (21) are shown in Figs. 3 and 4, respectively. Under the assumption of parity conservation, that is, $\alpha_{\Xi^-} = 0$ for $\Xi^- \to \Lambda\pi^-$ or $g_+^{\Xi^-} = 0$ for $\Xi_c^+(\lambda_1) \to \Xi^-(\lambda_2)\pi^+\pi^+$, the distributions turn to be constants. Otherwise, when parity violation exists, the absolute amplitudes of the distributions

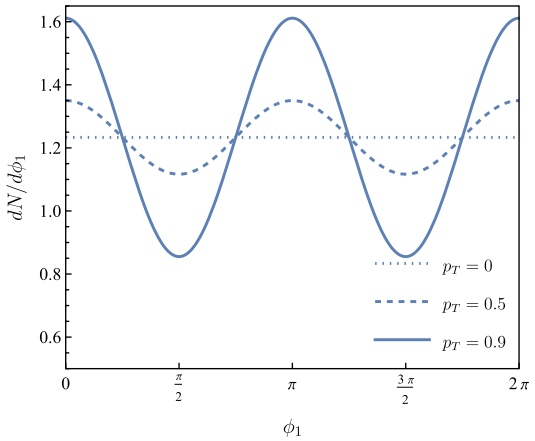

Fig. 3. (color online) Angular distributions of ϕ_1 for $p_T = 0$, 0.5, 0.9 (dotted, dashed, and solid lines, respectively).

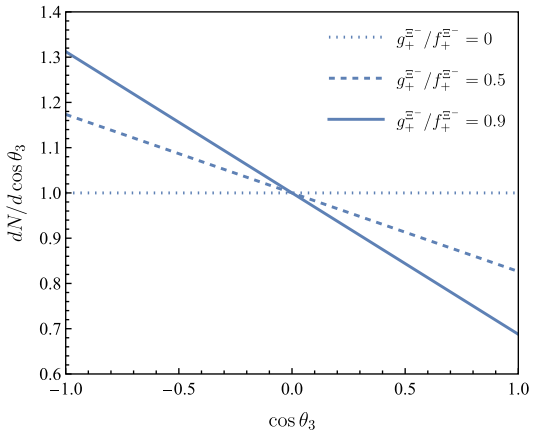

Fig. 4. (color online) Angular distributions of $\cos\theta_3$ for $g_+^{\Xi^-}/f_+^{\Xi^-} = 0$, 0.5, 0.9 (dotted, dashed, and solid lines, respectively).

for $\cos\theta_3$ are non-zero.

The angular distribution after normalization is defined as

$$\widetilde{\mathcal{W}} = \frac{\mathcal{W}(\theta_i,\phi_i,\alpha_i)}{\int \Pi_i^4 \mathrm{d}\cos\theta_i\phi_i \mathcal{W}(\theta_i,\phi_i,\alpha_i)}. \tag{23}$$

It is important to define the weighted polarizations of Ξ_c^+ depending on θ_1 or ϕ_1 by integrating out other angles:

$$\frac{\mathrm{d}\langle\mathcal{P}_0\rangle}{\mathrm{d}\cos\theta_1} \propto 1 + 2\alpha_c\cos^2\theta_1 + \alpha_c^2\left(\cos^4\theta_1 + \frac{p_T^4}{2}\sin^4\theta_1\right), \tag{24}$$

$$\frac{\mathrm{d}\langle\mathcal{P}_0\rangle}{\mathrm{d}\phi_1} \propto 1 + \frac{2}{3}\alpha_c(1 + 2p_T^2\cos 2\phi_1) + \frac{\alpha_c^2}{5}\left(1 + \frac{4}{3}p_T^2\cos 2\phi_1 + \frac{8}{3}p_T^4\cos^2(2\phi_1)\right), \tag{25}$$

$$\frac{\mathrm{d}\langle\mathcal{P}_y\rangle}{\mathrm{d}\phi_1} \propto (1 - p_T^2\cos 2\phi_1)\sin\phi_1, \tag{26}$$

$$\frac{\mathrm{d}\langle\mathcal{P}_x\rangle}{\mathrm{d}\phi_1} \propto p_T^2\sin 2\phi_1, \tag{27}$$

and $\mathrm{d}\langle\mathcal{P}_z\rangle/\mathrm{d}\phi_1 = 0$. The corresponding plots are shown in Figs. 5, 6, 7, and 8 respectively. The beam polarization enhances the polarizations distributions of ϕ_1 but suppresses the unpolarization distribution of $\cos\theta_1$.

For the observed data sample of N events, the likelihood function is expressed as [38]

$$L(\theta_i,\phi_i,\alpha_c,\alpha_{\Xi^-},\alpha_\Lambda,\alpha_{\Xi_c^+},\beta_{\Xi_c^+},\gamma_{\Xi_c^+}) = \prod_{i=1}^{N}\widetilde{\mathcal{W}}_j, \tag{28}$$

where θ_i and ϕ_i represent the polar and azimuthal angle; α_c, α_{Ξ^-}, α_Λ, $\alpha_{\Xi_c^+}$, $\beta_{\Xi_c^+}$, and $\gamma_{\Xi_c^+}$ represent the decay parameters; and the product is computed based on the probability of the i-th event $\widetilde{\mathcal{W}}_j$. Here, α_{Ξ^-} and α_Λ are fixed to PDG values [25]. According to the maximum likelihood method, the relative uncertainty for estimating statistical sensitivity to parity parameter $\alpha_{\Xi_c^+}$ is defined as

$$\delta(\alpha_{\Xi_c^+}) = \frac{\sqrt{V(\alpha_{\Xi_c^+})}}{|\alpha_{\Xi_c^+}|}, \tag{29}$$

where the inverse of the variance is given by

$$V^{-1}(\alpha_{\Xi_c^+}) = N\int \frac{1}{\widetilde{\mathcal{W}}}\left[\frac{\partial\widetilde{\mathcal{W}}}{\partial\alpha_{\Xi_c^+}}\right]^2 \prod_i^4 \mathrm{d}\cos\theta_i\mathrm{d}\phi_i. \tag{30}$$

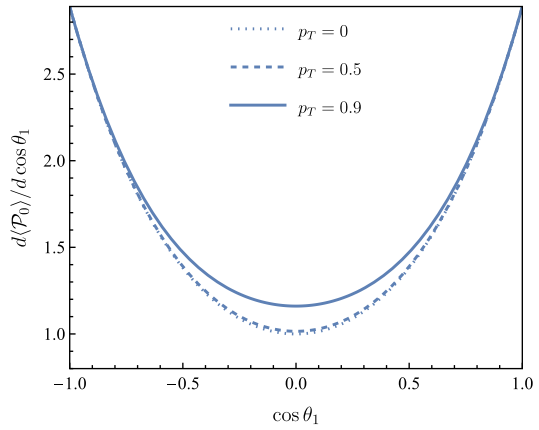

Fig. 5. (color online) Weighted $\mathcal{P}_0$ as a function of $\cos\theta_1$ for $p_T = 0$, 0.5, 0.9 (dotted, dashed, and solid lines, respectively).

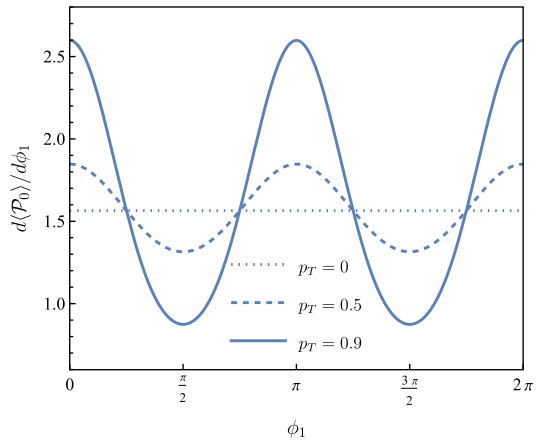

Fig. 6. (color online) Weighted $\mathcal{P}_0$ as a function of ϕ_1 for $p_T = 0$, 0.5, 0.9 (dotted, dashed, and solid lines, respectively).

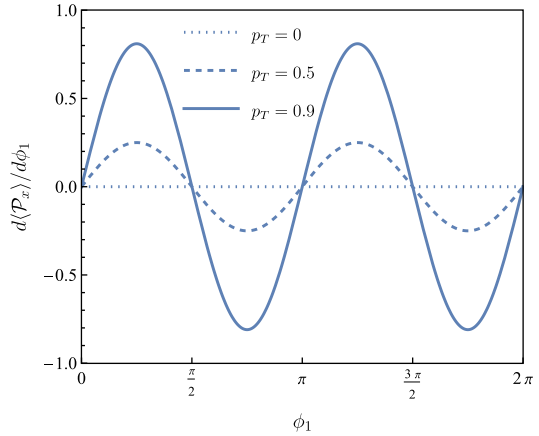

Fig. 7. (color online) Weighted $\mathcal{P}_x$ as a function of ϕ_1 for $p_T = 0$, 0.5, 0.9 (dotted, dashed, and solid lines, respectively).

Indeed, to identify the significance of CP violations, the statistical sensitivity of $\mathcal{A}_{\mathrm{CP}}$ in Eq. (4) can be estimated if $\alpha_{\Xi_c^+}$ and $\bar{\alpha}_{\Xi_c^-}$ are considered as non-correlation via the following error propagation formula:

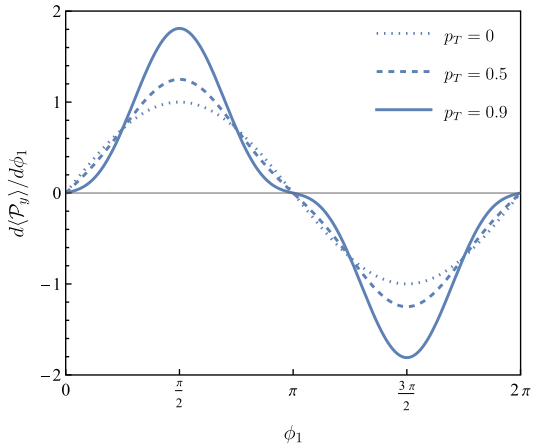

Fig. 8. (color online) Weighted $\mathcal{P}_y$ as a function of ϕ_1 for $p_T = 0,\ 0.5,\ 0.9$ (dotted, dashed, and solid lines, respectively).

$$\delta(\mathcal{A}_{\rm CP}) = \frac{2\sqrt{\alpha^2_{\Xi_c^+}\delta(\bar{\alpha}_{\bar{\Xi}_c^-})^2 + \bar{\alpha}^2_{\bar{\Xi}_c^-}\delta(\alpha_{\Xi_c^+})^2}}{(\alpha_{\Xi_c^+} - \bar{\alpha}_{\bar{\Xi}_c^-})^2}, \tag{31}$$

where $\delta(\bar{\alpha}_{\bar{\Xi}_c^-})$ is the sensitivity for the $\bar{\Xi}_c^-$ system. The sensitivities $\delta(\mathcal{B}_{\rm CP})$ and $\delta(C_{\rm CP})$ for the other two CP parameters can be defined similarly.

IV. NUMERICAL SENSITIVITIES

We are particularly interested in the dependence of statistical sensitivities on asymmetry parameters and beam polarizations. To clarify the analysis, we set $\alpha_c = 0.7$, $\Delta_1 = \pi/6$, and $\Delta_\pm = \Delta^+ = \pi/3$. We verified that other sets of phase angle values do not significantly affect the statistical quantities. In the following figures, when one parameter is varied, the other two parameters are held constant. For example, the red lines in Fig. 9 represent the distributions of $\delta(\alpha_{\Xi_c^+})$ as functions of the event number N, with $\beta_{\Xi_c^+} = 0.1$ and $\gamma_{\Xi_c^+} = 0.5$ fixed. Similarly, the blue lines represent the distributions of $\delta(\beta_{\Xi_c^+})$ with $\alpha_{\Xi_c^+} = 0.1$ and $\gamma_{\Xi_c^+} = 0.5$, while the green lines show the distributions of $\delta(\gamma_{\Xi_c^+})$ with $\alpha_{\Xi_c^+} = 0.1$ and $\beta_{\Xi_c^+} = 0.3$. These sensitivities exhibit a negative correlation with the absolute values of the parameters. Under our chosen parameter values at $\alpha_{\Xi_c^+} = 0.5$ and $\beta_{\Xi_c^+} = 0.5$, the corresponding sensitivities reach 1% for approximately 3×10^5 signal events.

In Fig. 9, the statistical significance of $\gamma_{\Xi_c^+}$ is weak with respect to $\alpha_{\Xi_c^+}$ and $\beta_{\Xi_c^+}$ under same signal events. However, $\delta(\gamma_{\Xi_c^+})$ exhibits a strong dependence on beam polarizations given that its parameter is defined as the radio of two projections of angular momentum in Eq. (1). As shown in Fig. 10, the measurement accuracy of $\gamma_{\Xi_c^+}$ can be improved through the beam polarization contribution. The significance of $\gamma_{\Xi_c^+}$ is also relative to intrinsic phase difference Δ_1 according to Eq. (10). If Δ_1 reaches the saddle point $\pi/2$, the requirement for events decreases apparently; the corresponding curves are shown in Fig. 11. In addition, the sensitivities of $\alpha_{\Xi_c^+}$ and $\beta_{\Xi_c^+}$ were found to be insensitive to p_T and Δ_1.

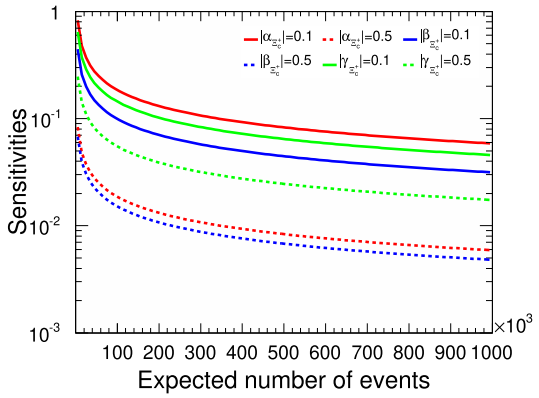

Fig. 9. (color online) $\alpha_{\Xi_c^+}$, $\beta_{\Xi_c^+}$, and $\gamma_{\Xi_c^+}$ sensitivity distributions relative to signal yields in terms of different parameters. The red solid and dashed lines represent the $\alpha_{\Xi_c^+}$ values of 0.1 and 0.5, respectively. The blue solid and dashed lines represent the $\beta_{\Xi_c^+}$ values of 0.1 and 0.5, respectively. The green solid and dashed lines represent the $\gamma_{\Xi_c^+}$ values of 0.1 and 0.5, respectively.

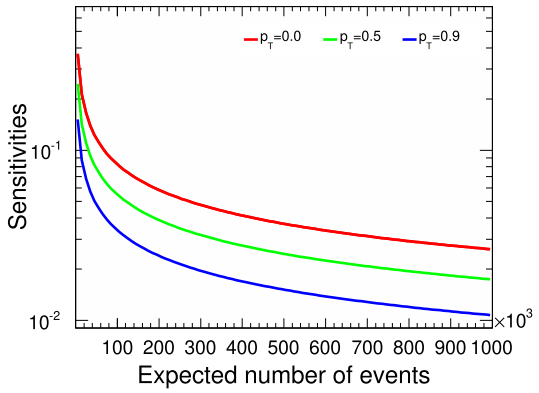

Fig. 10. (color online) $\gamma_{\Xi_c^+}$ sensitivity distribution relative to signal yields assuming $\gamma_{\Xi_c^+} = 0.5$. The p_T values of 0.0, 0.5, and 0.9 correspond to the red, green, and blue lines, respectively.

Next, let us consider the sensitivity estimation on the CP violation parameters in terms of the error propagation equation Eq. (31). The CP violation in the charm system should be weaker than that in the bottom system [13]; therefore, we constrained the upper limit of parameters, for example $\mathcal{A}_{\rm CP} < 0.05$; the plot for the sensitivity of this parameter is shown in Fig. 12, where the bands represent uncertainty. The statistical significances for P and CP violations are positively correlated, but the latter one requires more events to reach same sensitivities. For example, we found the parity sensitivity to be 0.01 when $N = 300000$, while the CP sensitivity was approximately 0.04 by comparing lines in Figs. 9 and 12 for $\alpha_{\Xi_c^+} = 0.5$. The variations of $\mathcal{B}_{\rm CP}$ and $C_{\rm CP}$ sensitivities on different

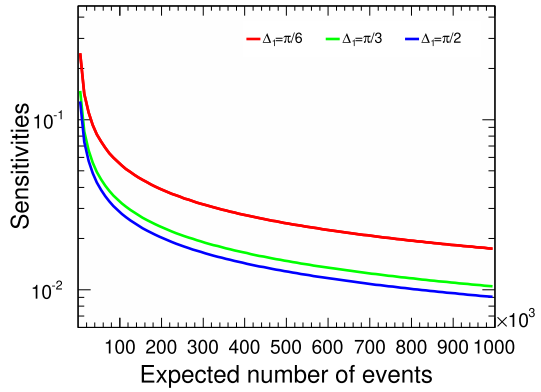

Fig. 11. (color online) $\gamma_{\Xi_c^+}$ sensitivity distributions relative to signal yields assuming $\gamma_{\Xi_c^+}=0.5$. The Δ_1 values of $\pi/6$, $\pi/3$, and $\pi/2$ correspond to the red, green, and blue lines, respectively.

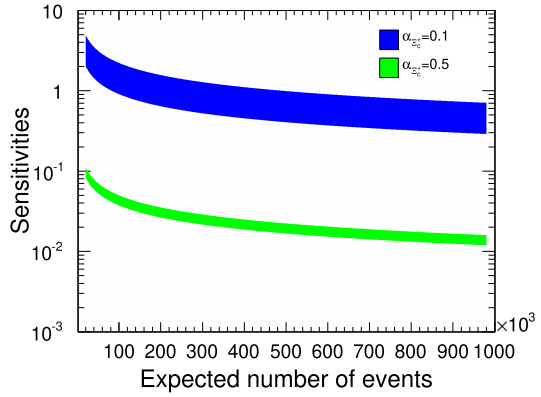

Fig. 12. (color online) $\mathcal{A}_{\rm CP}$ sensitivity distributions relative to signal yields. The $\alpha_{\Xi_c^+}$ values of 0.1 and 0.5 correspond to the blue and green bands, respectively.

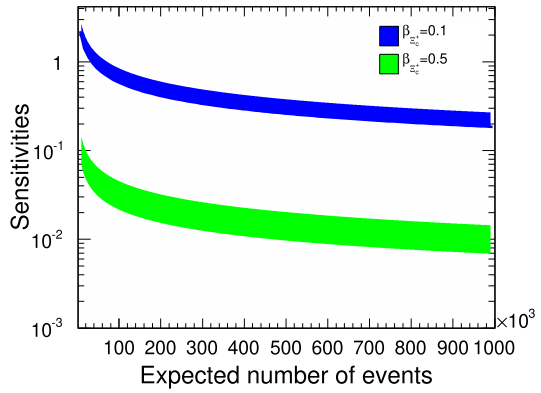

Fig. 13. (color online) $\mathcal{B}_{\rm CP}$ sensitivity distributions relative to signal yields. The $\beta_{\Xi_c^+}$ values of 0.1 and 0.5 correspond to the blue and green bands, respectively.

parameters are shown in Figs. 13 and 14, respectively. It is also demonstrated in Fig. 15, that, at a fixed significance level, higher polarization reduces the number of events needed to achieve a given sensitivity to $C_{\rm CP}$ sensitivity.

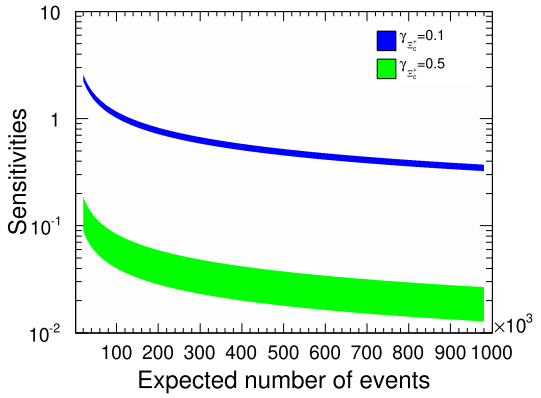

Fig. 14. (color online) $C_{\rm CP}$ sensitivity distributions relative to signal yields. The $\gamma_{\Xi_c^+}$ values of 0.1 and 0.5 correspond to the blue and green bands, respectively.

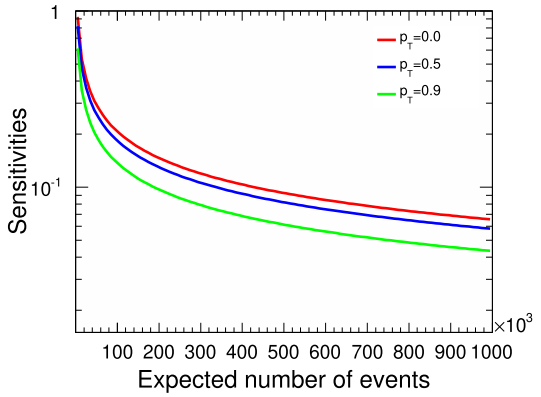

Fig. 15. (color online) $C_{\rm CP}$ sensitivity distributions relative to signal yields assuming $\gamma_{\Xi_c^+}=0.5$. The red, blue, and green lines represent the p_T values of 0.0, 0.5, and 0.9, respectively.

V. SUMMARY

The Cabibbo-favored three-body decay processes $\Xi_c^+\to\Xi^0\pi^+\pi^0$ and $\Xi_c^+\to\Xi^-\pi^+\pi^+$ represent the most probable decay modes of Ξ_c^+. The intermediate processes $\Xi_c^+\to\Xi(1620)^0\pi^+\to\Xi^-\pi^+\pi^+$ and $\Xi_c^+\to\Xi(1690)^0\pi^+\to\Xi^-\pi^+\pi^+$ can also be measured with same method. By measuring the asymmetry decay parameters, the P and CP symmetries can be systematically tested. With sufficiently large data samples, the precision of the decay parameters $\alpha_{\Xi_c^+}$, $\beta_{\Xi_c^+}$, and $\gamma_{\Xi_c^+}$ can be significantly improved. Notably, For a given data sample, the statistical significance increases as the decay parameter approaches its theoretical extremes (±1). Experimentally, there are some challenges in achieving controllable beam polarization. However, the effect of beam polarization can significantly enhance the precisions of $\gamma_{\Xi_c^+}$ and $\mathcal{A}_{\rm CP}$ measurements. Therefore, it is critical to achieve a controllable beam polarization in future experiments, especially for a precise study of CP. For instance, when the phase differ-

ence Δ_1 is close to $\pi/2$, and decay parameters are close to 1, the sensitivity becomes more evident. The expected CP violation in $\Xi_c^+ \to \Xi^-\pi^+\pi^+$ decay from weak interactions is on the order of 10^{-4} to 10^{-5}, which means suppresion with respect to an approximate benchmark number of 10^{-3} [39]. Measurements of $\mathcal{A}_{\rm CP}$ and $\mathcal{B}_{\rm CP}$ will provide a suitable constraint to the total CP violation in this decay. Therefore, it is estimated that at least 1.0×10^9 $\Xi_c^+\bar{\Xi}_c^-$ events are required to observe CP violation, under the assumption of $\alpha_{\Xi_c^+} = 0.5$. The process could serve as an excellent probe to search for new sources of CP violation beyond the Standard Model. In this study, the sensitivities to the asymmetry parameters and to CP violation for the decay $\Xi_c^+ \to \Xi^-\pi^+\pi^+$ were evaluated under various data sample sizes and beam polarization conditions. This study constitutes the first investigation of P and CP violations in the three-body decay of Ξ_c^+, providing essential theoretical support for future experiments, such as STCF.

References

[1] A. D. Sakharov, Pisma Zh. Eksp. Teor. Fiz. **5**, 32 (1967)
[2] N. Cabibbo, Phys. Rev. Lett. **10**, 531 (1963)
[3] M. Kobayashi and T. Maskawa, Prog. Theor. Phys. **49**, 652 (1973)
[4] J. H. Christenson, J. W. Cronin, V. L. Fitch *et al.*, Phys. Rev. Lett. **13**, 138 (1964)
[5] A. Abashian *et al.* (Belle Collaboration), Phys. Rev. Lett. **86**, 2509 (2001)
[6] B. Aubert *et al.* (BaBar Collaboration), Phys. Rev. Lett. **86**, 2515 (2001)
[7] Y. Chao *et al.* (Belle Collaboration), Phys. Rev. Lett. **93**, 191802 (2004)
[8] B. Aubert *et al.* (BaBar Collaboration), Phys. Rev. Lett. **93**, 131801 (2004)
[9] R. Aaij *et al.* (LHCb Collaboration), Phys. Rev. Lett. **122**, 211803 (2019)
[10] H. N. Li, C. D. Lü, and F. S. Yu, arXiv: 1903.10638 [hep-ph]
[11] M. E. Peskin, Nature **419**, 24 (2002)
[12] R. Aaij *et al.* (LHCb Collaboration), Phys. Rev. Lett. **134**, 101802 (2025)
[13] R. Aaij *et al.* (LHCb Collaboration), Nature **643**, 1223 (2025)
[14] T. D. Lee, J. Steinberger, G. Feinberg *et al.*, Phys. Rev. **106**, 1367 (1957)
[15] M. Ablikim *et al.* (BESIII Collaboration), Nature **606**, 64 (2022)
[16] M. Ablikim *et al.* (BESIII Collaboration), Phys. Rev. Lett. **129**, 131801 (2022)
[17] M. Ablikim *et al.* (BESIII Collaboration), Phys. Rev. Lett. **131**, 191802 (2023)
[18] M. Ablikim *et al.* (BESIII Collaboration), Phys. Rev. Lett. **125**, 052004 (2020)
[19] M. Ablikim *et al.* (BESIII Collaboration), arXiv: 2503.17165 [hep-ex]
[20] J. Tandean, Phys. Rev. D **69**, 076008 (2004)
[21] N. Salone, P. Adlarson, V. Batozskaya *et al.*, Phys. Rev. D **105**, 116022 (2022)
[22] X. G. He, J. Tandean, and G. Valencia, Sci. Bull. **67**, 1840 (2022)
[23] X. G. He, H. Murayama, S. Pakvasa *et al.*, Phys. Rev. D **61**, 071701 (2000)
[24] E. Goudzovski, D. Redigolo, K. Tobioka *et al.*, Rept. Prog. Phys. **86**, 016201 (2023)
[25] S. Navas *et al.* (Particle Data Group), Phys. Rev. D **110**, 030001 (2024)
[26] M. Achasov, X. C. Ai, R. Aliberti *et al.*, Front. Phys. (Beijing) **19**, 14701 (2024)
[27] T. D. Lee and C. N. Yang, Phys. Rev. **108**, 1645 (1957)
[28] S. U. Chung, (1971), 10.5170/CERN-1971-008
[29] M. Mikhasenko *et al.* (JPAC), Phys. Rev. D **101**(3), 034033 (2020)
[30] J. P. Wang and F. S. Yu, Phys. Lett. B **849**, 138460 (2024)
[31] J. F. Donoghue, X. G. He, and S. Pakvasa, Phys. Rev. D **34**, 833 (1986)
[32] M. Saur and F. S. Yu, Sci. Bull. **65**, 1428 (2020)
[33] M. G. Doncel, P. Mery, L. Michel *et al.*, Phys. Rev. D **7**, 815 (1973)
[34] H. Chen and R. G. Ping, Phys. Rev. D **102**, 016021 (2020)
[35] X. Cao, Y. T. Liang, and R. G. Ping, Phys. Rev. D **110**, 014035 (2024)
[36] M. Ablikim *et al.* (BESIII Collaboration), Phys. Lett. B **770**, 217 (2017)
[37] D. H. Wei, Y. X. Yang and R. G. Ping, Chin. Phys. C **46**(7), 074002 (2022)
[38] T. Z. Han, R. G. Ping, T. Luo *et al.*, Chin. Phys. C **44**, 013002 (2020)
[39] S. Bianco, F. L. Fabbri, D. Benson *et al.*, Riv. Nuovo Cim. **26**(7-8), 1 (2003)